Passive Control of Tall Buildings Using Distributed Multiple Tuned Mass Dampers

Hamid Radmard Rahmani*, Carsten Könke

Institute of Structural Mechanics, Bauhaus-Universität Weimar, Marienstr. 15, D-99423 Weimar, Germany

Abstract

The vibration control of the tall building during earthquake excitations is a challenging task due to their complex seismic behavior. This paper investigates the optimum placement and properties of the Tuned Mass Dampers (TMDs) in tall buildings, which are employed to control the vibrations during earthquakes. An algorithm was developed to spend a limited mass either in a single TMD or in multiple TMDs and distribute them optimally over the height of the building. The Non-dominated Sorting Genetic Algorithm (NSGA – II) method was improved by adding multi-variant genetic operators and utilized to simultaneously study the optimum design parameters of the TMDs and the optimum placement. The results showed that under earthquake excitations with noticeable amplitude in higher modes, distributing TMDs over the height of the building is more effective in mitigating the vibrations compared to the use of a single TMD system. From the optimization, it was observed that the locations of the TMDs were related to the stories corresponding to the maximum modal displacements in the lower modes and the stories corresponding to the maximum modal displacements in the modes which were highly activated by the earthquake excitations. It was also noted that the frequency content of the earthquake has significant influence on the optimum location of the TMDs.

Keywords: tall buildings, tuned Mass Dampers, genetic algorithm, binary coding, structural control

1. Introduction

Given the modern development plans of large cities, which are designed to answer the needs of their fast-growing population, it is anticipated that the buildings in such cities will become taller and more expensive [1]. As result, the area of investigating solutions to provide safety and serviceability of tall

*Corresponding author
Email address: radmard.rahmani@gmail.com (Hamid Radmard Rahmani)

buildings in case of natural hazards such as strong winds and earthquakes has gained much attention in the last decade.

The current seismic design codes allow the structures to undergo inelastic deformations during strong earthquakes. Such structures would experience larger deformations but less seismic forces; otherwise, the structure should sustain much larger earthquake loads.

On the other hand, the deformations under wind and earthquake loads are limited due to stability and serviceability provisions. The resultant structures are stiff enough to withstand the wind loads, without forming noticeable deformations, while simultaneously being ductile enough to withstand strong earthquakes by adopting nonlinear behaviors.

However, particularly for controlling the vibrations in tall buildings, the code-based approaches don't necessarily lead to an applicable and affordable solution, as these structures need to withstand much larger wind and earthquake loads even though they have much lower lateral stiffness compared to low- and mid-rise buildings. Moreover, due to their very high construction costs, they are usually designed to endure for longer time periods, which increases their risk of experiencing strong earthquakes over the course of their service life.

A modern answer to these issues is the idea of structural control systems that include a variety of techniques, which can be classified into four main categories: passive, active, semi-active, and hybrid.

From a historical point of view, passive control systems such as base isolations and Tuned Mass Dampers (TMDs) were the first of these techniques to be implemented. Considerable research has focused on the passive controller systems, and they are already utilized in many countries [2, 3]. As these systems need no external power supply, they are easier to implement and design, when compared to other advanced controllers.

The concept of TMDs was first applied by Frahm in 1909 [4] to mitigate the rolling motions in ships. Since then, many researches have been conducted on TMDs, and they have been widely utilized in vibration control systems. In structural control problems, TMDs have been successfully implemented in different structures such as bridges [5, 6] and buildings [7, 8, 9, 10, 11, 12] to reduce earthquake- and wind- induced vibrations. Observations of TMDs show that they can effectively reduce vibrations in structures that are excited by high winds, high-speed trains, and traffic loads and also help decrease the discomfort of the inhabitants during minor earthquakes [13, 14, 6].

As single TMD systems can be tuned to a particular frequency, they are very sensitive to mistuning and uncertainties. As a solution, Multiple Tuned Mass Dampers (MTMDs) were first introduced by Igusa and Xu in 1990 [15], after which they have been studied in several researches [16, 17, 9, 10, 18, 19, 12, 20]. Li et al. [21] considered the structure as a Single Degree of Freedom (SDOF) system, when connected to multiple TMDs, and studied the optimum design parameters for those TMDs. With respect to using MTMD systems in multi-story buildings, Chen et al. [9] studied the efficiency of using multiple TMDs in mitigating the seismic responses in a six-story building. After that, Tharwat [16] used partial floor loads as MTMDs. These researches show that the MTMD

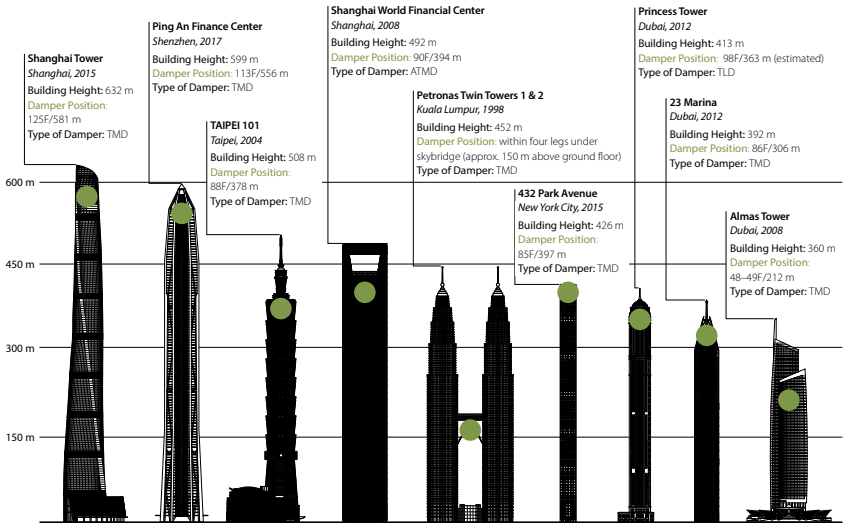

Figure 1: Tallest completed buildings with dampers[22]

systems cover a wider frequency range and are less sensitive to the uncertainties of the system.

In addition to multi-story buildings, several tall buildings have benefited from the utilization of TMDs in controlling their vibrations (see Figure 1).

As has been shown, most of them are equipped with a single TMD, which is placed in the top level of the building. The studies also showed that using a single TMD in the top levels of the tall buildings can effectively reduce wind-induced motions [23, 24]. This is because the structures respond to the wind excitation with respect to their first structural mode in which the top levels of the building have maximum modal displacement. Therefore, placing a single TMD on the top level with a tuning frequency closer to the fundamental structural frequency can efficiently reduce the structural responses. In another research, Elias et al. [10] studied the use of distributed MTMD systems in reducing wind-induced vibrations in a tall building. They concluded that the distributed MTMDs are more effective, as compared to a single TMD system and an MTMD system in which all the TMDs are placed on the top level.

The researches show that TMDs are also effective in mitigating earthquake vibrations in the buildings. Arfiadi et al. [7] used a hybrid genetic algorithm method to find the optimum properties and the location of a TMD for a 10-story building under earthquake excitation. In another research, Pourzeinali et al. [25] utilized multi-objective optimization to outline the design parameters of a TMD in a 12-story building under earthquake excitation. Li proposed a novel optimum criterion to optimize the properties of double TMDs for structures

under ground acceleration.[12].

In all the researches about tall buildings cited here, either the parameters of the TMDs have mainly been studied under wind-induced vibrations or a single TMD has been studied under earthquake excitation; currently, studying the optimum parameters of TMDs under earthquake excitation, without limiting the number and location of the TMDs, is still a challenging task, because of the stochastic nature of the earthquakes and the complex seismic behavior of such buildings, which mandate extensive and thorough studies.

Additionally, in contrast to the wind loads, during the earthquakes, the higher modes may have more noticeable participation in the total response of tall buildings. This is mainly because of the (1) low frequency of the higher modes in these structures, compared to low- and mid-rise buildings, and (2) the wide frequency content of the earthquakes that may activate the multiple modes in such buildings. Therefore, only controlling the lower modes by placing TMDs on the top levels would not necessarily lead to the optimum solution for controlling the motions in these buildings during earthquakes.

1.1. Problem definition

This paper addresses the mentioned issues by studying the optimum placement and properties of TMDs in a 76-story benchmark building as case study which is subjected to seven scaled earthquake excitations. The variables of the resultant optimization problem include the positions and properties of the TMD. The goal of the optimization is to reduce the controlled-to-uncontrolled ratio of the displacement, velocity, and acceleration seismic responses. In order to solve such multi-objective optimization problem, an improved revision of the *Non-dominated Sorting Genetic Algorithm (NSGA II)* is developed and utilized.

In each loop, the algorithm generates an arrangement and properties of the TMDs using the NSGA-II method, and sends it to the *analyzer module* to determine the responses of the building equipped with such a TMD arrangement under different earthquake excitations. Based on the responses, the algorithm assigns a fitness value for such TMD arrangements. The fitness value is an index that shows how good or bad the obtained responses are.The NSGA-II then utilizes a refined history of the TMD arrangements and corresponding fitness values for its next suggestion in the next loop. In this study, the algorithm was allowed to spend an applicable mass in a single TMD or distribute it through multiple TMDs over the height of the building.

1.2. Contributions

This research incorporates several contributions in the field of passive control of tall buildings and optimization problems. First, the issues with a single TMD system in controlling tall buildings are addressed, and improvements are proposed by studying multi-mode control via distribution of the TMDs over the height of the building. Likewise, it investigates how the frequency content of the earthquake can affect the optimum position and properties of the TMDs. Moreover, the performance of the NSGA-II algorithm is enhanced by adding

multi-variant genetic operations, and the resulting algorithms are presented. Finally, the optimum hyper parameters of the genetic algorithm for tackling similar problems is proposed by performing sensitivity analysis.

1.3. Outlines

The mathematical settings of a structural dynamic problem are mentioned in Section 2. Then the utilized algorithms, including the Genetic Algorithm (GA) and the NSGA-II method, are described in Sections 3 and 4. After that, the case study is presented in Section 5, and the selection and scaling of the earthquakes are noted. Then, the results of the sensitivity analysis of the GA hyper parameters for optimizing the performance of the GA algorithm are presented; the optimization process is then detailed in Section 9. Finally, the obtained results are presented and discussed in the Sections 10 and 11, and the relevant conclusions are drawn.

2. Mathematical model of the building

The governing equation of the motion of a tall building under earthquake excitation is as follows:

$$[M]\left\{\ddot{U}\right\} + [C]\left\{\dot{U}\right\} + [K]\{U\} = \{P_t\} \tag{1}$$

where, M, K and C represent the mass, the stiffness and the damping matrices of the structure and the TMDs:

$$[M] = [M_{st}] + [M_t] \tag{2}$$

$$[C] = [C_{st}] + [C_t] \tag{3}$$

$$[K] = [K_{st}] + [K_t] \tag{4}$$

Indexes st and t indicate the Degrees of Freedom (DOFs) of the building and the TMDs, respectively.

The external load vector, P_t, in Eq. 1 comprises inertial forces due to ground acceleration as follows:

$$\{P_t\} = -\ddot{u}_g\,[M]\,\{1_t\} \tag{5}$$

where $\{1_t\}_{(N+n)\times 1} = [1\,1\,\cdots\,1]^T$ and the term $\ddot{u}_g$ represents the ground accelerations.

The structural responses, including displacement, velocity, and acceleration matrices, can be expressed as follows:

$$\{U\} = \{u_{st1}, u_{st2}, \ldots, u_{stN}, u_{t1}, u_{t2}, \ldots, u_{tn}\} \tag{6}$$

$$\{V\} = \{v_{st1}, v_{st2}, \ldots, v_{stN}, v_{t1}, v_{t2}, \ldots, v_{tn}\} \tag{7}$$

$$\{A\} = \{a_{st1}, a_{st2}, \ldots, a_{stN}, a_{t1}, a_{t2}, \ldots, a_{tn}\} \tag{8}$$

In these equations, N and n represent the number of degrees of freedom (DOF) for the building and the TMDs respectively. Therefore, the dimensions of the M, K and C matrices are $(N+n) \times (N+n)$.

The design parameters of a TMD include its damping, tuning frequency, and mass. Generally, the ratios of these parameters to the corresponding values of the structures have more importance and are utilized in the design procedures:

$$m_0 = \frac{m_t}{m_{st}}, \beta = \frac{\nu_t}{\nu_{st}}, \psi = \frac{c_t}{c_{st}} \tag{9}$$

The parameters m_0, β, ψ refer to mass, frequency, and damping ratios, while the indexes t and st indicate the TMD and the structural properties.

In order to solve the equations of the motion in this study, Newmark's β method is utilized. The average acceleration method is considered by setting $\gamma = \frac{1}{2}$ and $\beta = \frac{1}{4}$ in the relevant formulation[26].

3. Genetic Algorithm

Genetic Algorithm (GA) is a nature-inspired method within a larger family of methods called *evolutionary optimization methods*. Genetic algorithms rely on bio-inspired operators, such as mutation, crossover, and selection, to search the solution space and find an optimum solution regarding the fitness function [27].

3.1. Elements of Genetic Algorithm

In the GA method, a *population* of the solutions, called *individuals*, to an optimization problem is evolved toward better solutions. Each candidate solution has a chromosome consisting of an encoded set of variables.

The evolution usually starts from a random population and proceeds as an iterative process of performing genetic operations on the individuals to produce new members, while selecting the elite members to form new generations. The new generation of solutions is then used in the next iteration of the algorithm. Generally, the termination criteria involve either reaching a maximum number of generations or a desired fitness value[28].

- **Encoding**

In GA, the solutions are represented by encoding the variables. One of the commonly used encoding techniques is binary encoding in which the variables are coded to strings of 0s and 1s to form the chromosomes.

- **Selection**

During each successive generation, a portion of the existing population is selected to breed a new generation. Individual solutions are selected through a fitness-based process, where fitter solutions are typically more likely to be selected.

- **Fitness**

The fitness function quantifies the quality of the represented solutions. In multi-objective problems, the fitness function includes some sub-functions, each related to a particular objective.

- **Genetic operators**

These include crossover and mutation. In the crossover operation, the algorithm exchanges some of one parent's genes with those of the other, and in the mutation, it changes some genes of one parent [29, 30, 31, 32, 33].

4. Fast and Elitist Multi-Objective Genetic Algorithm NSGA-II

4.1. Introduction

In this paper, the NSGA-II method [34] is utilized to investigate the optimum arrangement and properties of TMDs in a tall building. NSGA-II is a non-domination based genetic algorithm invented for multi-objective optimization problems. In this method, the initial population is randomly generated, as in a normal GA procedure, and then the algorithm sorts the population with respect to the *non-domination rank* and the *crowding distance*.

1. **Non-domination rank**

In general, X dominates Y if X is no worse than Y in all the objectives and if X is better than Y in at least one objective. In the next step, the non-dominant set in the population is selected as the first front. The second front contains the sets that are only dominated by the first front sets. This procedure continues until all the members in the population have been categorized into different fronts. The fronts are then sorted from the first to the last. Figure 2 shows an illustration of solutions belonging to different ranks[35].

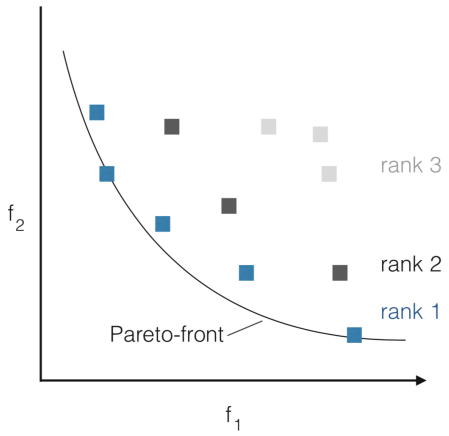

Figure 2: Non-dominated sorting of solutions[35]

2. **Crowding distance**

Among the non-dominated solutions or a union of the first ranks of non-dominated solutions, NSGA-II seeks a broad coverage. This is achieved with the crowding distance, which is the Manhattan distance between the left and right neighboring solutions for two objectives, as shown in Figure 3.

Consequently, each solution that cannot be dominated by other solutions and has a larger crowding distance than the others will obtain the first rank and so on.

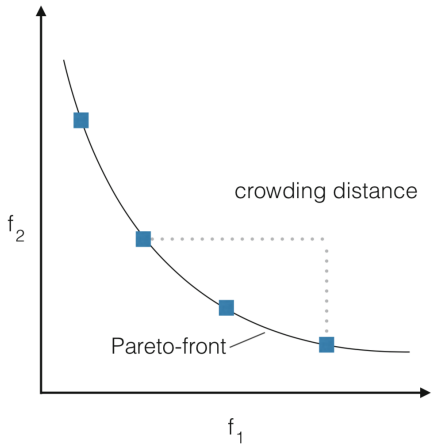

Figure 3: Illustration of crowding distance[35]

4.2. Repair

The repair method makes infeasible solutions feasible. Figure 4 schematically shows the repair approach for a solution space with an infeasible solution and two solutions in the feasible region. In this research, an infeasible solution includes the out-of-limit properties for TMDs. As is shown, the repair function would project each of these infeasible solutions to the closest feasible solution. The developed repair function calculates the shortest distance of the TMD properties(m_0, β, ψ) in the infeasible solution and corrects the chromosome with respect to the calculated distance (see Algorithm 1).

Algorithm 1 Repair individuals

```
procedure REPAIR(individual)
    st = DECODER(individual)
    for each tmd in st
        for each property in tmd
            if not property in acceptableRange
                property = CLOSESTINRANGE(property)
            end if
        tmd = RENEW(tmd, property)
        end for
    newIndividual = CODER(st)
    end for
    return newIndividual
end procedure
```

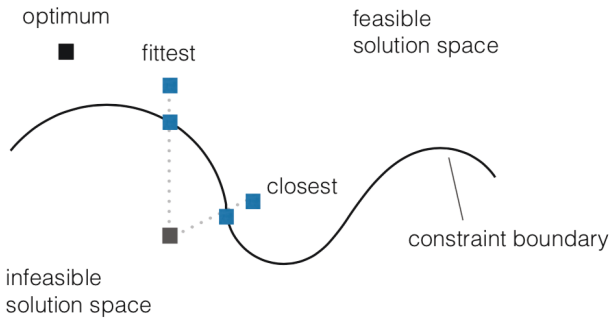

Figure 4: Repair of a infeasible solution[35]

4.3. Selection

The objective of selection is to choose the fitter individuals in the population to create off-springs for the next generation and then place them in a group commonly known as the mating pool. The mating pool is then subjected to further genetic operations that result in advancing the population to the next generation and hopefully closer to the optimal solution. In this research, the roulette wheel selection method was utilized for developing the selector function. As is also shown in Algorithm 2, the algorithm selects the individuals based on a probability proportional to the fitness. As is schematically illustrated in Figure 5, the principle of roulette selection is a linear search through a roulette wheel with the slots in the wheel weighted in proportion to the individual's fitness values. All the chromosomes (individuals) in the population are placed on the roulette wheel according to their fitness value[36]. In this algorithm, a probability value is assigned to each individual in the population. Based on these probabilities, the ranges [0,1] are divided between the individuals so that each individual obtains a unique range. The winning individual is then selected by generating a random number between zero and one and finding the individual whose range includes this random number.

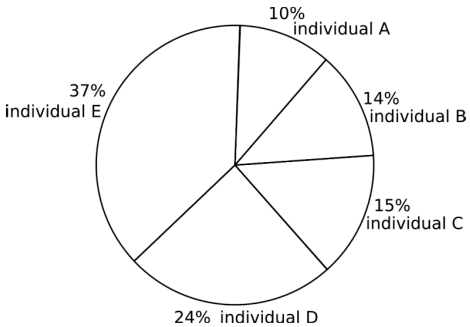

Figure 5: Roulette wheel selection

Algorithm 2 Making individual selection

```
procedure MakingSelection(population)
    fitPop = Fitness(population)
    sumFit = Sum(fitPop)
    percentFit = fitPop / sumFit
    rangeFitAdded = AddRange(fitPop, percentFit)
    randN= RND(1)
    for each individual in population
        r= rangeFitAdded(individual)
        if randN in range r
            selectedIndv = individual
            exit
        end if
    end for
    return selectedIndv
end procedure
```

In this algorithm, the *ADDRANGE* function, assigns a range to each individual based on its fitness values and its position on the wheel and the *RND (1)* function generates a random value between zero and one.

4.4. Optimization variables

In this study, three variables were defined to be optimized by the NSGA algorithm. As is schematically shown in Figure 6, the variables were as follows:

1. Number of TMDs
2. Position of the TMDs→ story number
3. TMDs' properties→ m_0, β, ψ

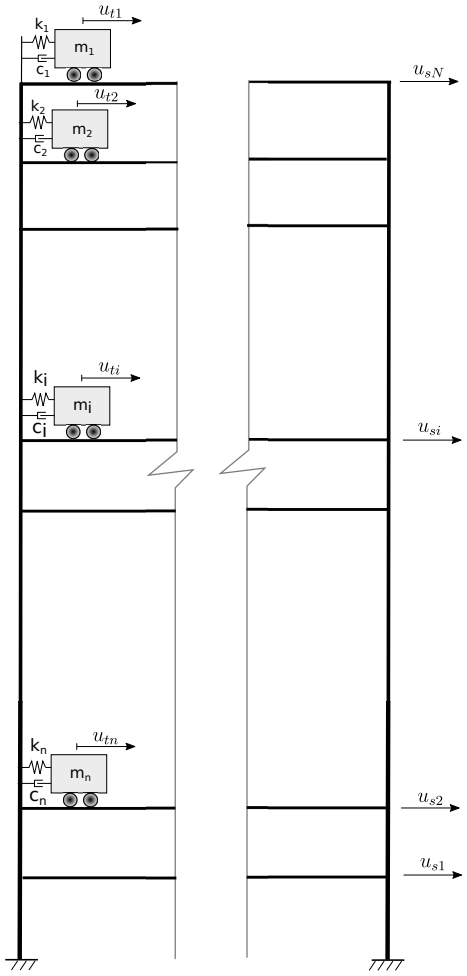

Figure 6: Building equipped by TMDs

4.5. Encoding

In this research, binary coding has been considered for creating genes. Therefore, the design variables of each TMD are coded into a binary string with a constant number of genes, as is shown in Figure 7. Each offspring contains the design parameters for the TMD as follows:

$$m_0 = \frac{m_t}{m_{st}}, \beta = \frac{\nu_t}{\nu_{st}}, \xi = \frac{c_t}{c_{st}} \tag{10}$$

where the t and st indexes correspond to the TMD and the structure respectively.

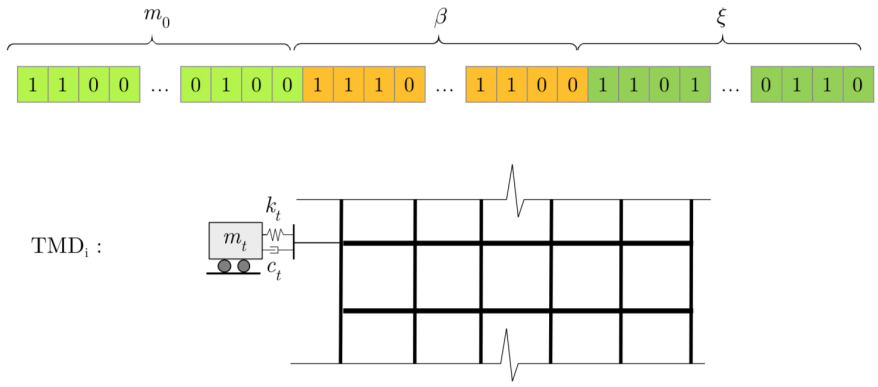

Figure 7: Binary coding the TMD's properties

After developing the genes for each TMD, the chromosomes are then created by combining all genes for each solution. As a result, each chromosome contains the coded data of all TMDs in the building. Using this definition, the position of each TMD is presented by the position of the related genes in the chromosome.

4.6. Genetic operators

a.Crossover function

In the crossover operation, two selected parents exchange random parts of their chromosome to create new off-springs. An appropriate strategy for selecting locations of the split points and the length of the transferred genes depends on the problem characteristics that highly affect the performance of the algorithm and the quality of the final results.

In this regard, different alternatives have been studied in this research to develop an appropriate crossover function. Examples of crossover operation forms that have been utilized in other researches but were not appropriate for this research are discussed as follows:

1. Single/k-point crossover - random points in whole chromosome:

In the initial steps, completely random selection of the genes for crossover has been considered as a commonly used crossover function. In this crossover type, after the parents are nominated by the algorithm, one or k points in the chromosome are randomly selected and the new off-springs are created by splitting and combining the parent chromosomes at the selected points. This process has often resulted in producing too many meaningless and low-quality off-springs, consequently reducing the performance of the algorithm dramatically. Examples of meaningless off-springs can include TMDs without one or more than one properties (e.g. without mass or stiffness).

2. Single/k-point crossover - random points in TMD genes:

Preventing the production of meaningless off-springs, the crossover function was improved in this study so that the genes related to the TMDs in each parent could be selected for performing a k-point crossover. Although the chances of creating meaningless off-springs were noticeably reduced, the performance of the algorithm was still not acceptable. The results showed that the efficiency of the operator in improving the results was not acceptable, as following this process, all the genes within the considered range for a TMD would be subjected to the same operations regardless of the genes' positions.

As an example, the genes related to the stiffness of a TMD in a parent were exchanged with those related to the damping properties in another parent, which is not logical. As a result, despite its improvements compared to the first form, the second crossover type leads to a very low convergence rate due to production of low-quality off-springs. In addition, one possible shortcut for reaching an optimum solution was missed; this step involves attaching the TMD of one parent to a story in another parent.

However, the maximum convergence rate obtained by developing a two-variant crossover function is presented in Algorithm 3. As is shown, in this function, in each call, one of the two developed crossover variants would be selected randomly. These variants are described as follows:

- Variant 1: In the first variation, the crossover operator acts on the parameters of the TMDs separately using the k-point crossover method, meaning that in each call, the crossover operator acts on the stiffness, mass or damping of the parents and exchanges the related properties using the k-point crossover function. The produced off-springs have TMDs in the same locations as their parents, but with different properties. Investigation of the performance of this function showed that this variant improves the properties of the TMDs regardless of their positions.

- Variant 2: The second crossover variation acts on the location of TMDs in the parents. The resultant off-springs include TMDs with the same properties as their parents but in other stories. These two crossover variations are demonstrated in Figure 8.

Algorithm 3 Crossover operator

procedure CrossOver(individual1, individual2)
    if rnd(1) < 0.5
        rndTmd1 = RandomSelect TMD **in** individual1
        rndTmd2 = RandomSelect TMD **in** individual2
        k = rndint(3)
        tmd1New = K-PointCrossover(rndTmd1)
        tmd2New = K-PointCrossover(rndTmd2)
        offspring1 = Rebuild(individual1, tmd1New)
        offspring2 = Rebuild(individual2, tmd2New)
    else
        rndTmd1 = randomselect TMD **in** individual1
        rndTmd2 = RandomSelect TMD **in** individual2
        tmd1New = rndTmd2
        tmd2New = rndTmd1
        offspring1 = Rebuild(individual1, tmd1New)
        offspring2 = Rebuild(individual2, tmd2New)
    end if
    return (offspring1, offspring2)
end procedure

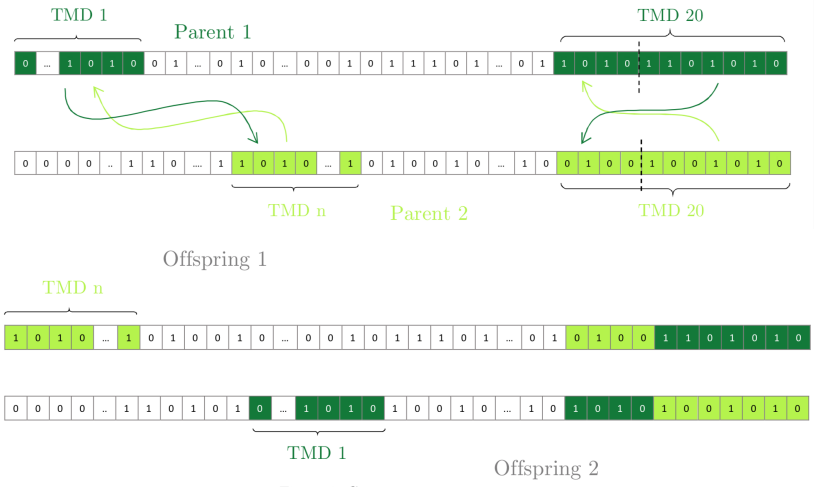

Figure 8: Crossover types

b.Mutation function

In the genetic algorithm, the mutation operator randomly changes one or multiple genes of a parent to produce new off-springs. Generally, in the binary coded chromosome, the following function is utilized to change the genes:

$$BinaryMutation(gen) = \begin{cases} 1 & if\ gen\ value = 0 \\ 0 & if\ gen\ value = 1 \end{cases}$$

In GA problems, the mutation function helps the algorithm to explore the solution space more broadly and prevents it from sticking to the local minimums. In addition, a proper mutation function improves the convergence speed. In this research, in order to to develop an appropriate mutation function, different variants were studied. It is understood that developing the mutation function without considering the characteristics of the problem would result in producing meaningless off-springs. Keeping this in mind, a two-variant mutation function was developed, which acted on the (1) genes related to TMD properties and (2) the group of genes related to the location of the TMDs.

Algorithm 4 Mutation operator

```
procedure MUTATION(individual)
    if rnd(1) < 0.5
        rndTmd = RANDOMSELECT TMD in individual
        newStory = rndint(76)
        tmdNew = MOVETMD(rndTmd, newStory)
        offspring = REBUILD(individual, tmdNew)
    else
        rndTmd = RANDOMSELECT TMD in individual
        targetGenCount = rndint(10)
        for i=1 to targetGenCount
            targetGen = RANDOMSELECTGEN(rndTmd)
            mutTmd = BINARYMUTATION(rndTmd, targetGen)
        end for
        offspring = REBUILD(individual, tmdNew)
    end if
    return (offspring)
end procedure
```

4.7. Fitness function

During the GA procedure, each solution comprised an arrangement of TMDs with different properties. In order to evaluate an individual solution, three objective functions were defined to shape the fitness function. The objectives of the optimization were taken to be the maximum ratios of displacement, velocity, and acceleration responses in controlled condition to their uncontrolled values as follows:

$$J_1 = max. \left(\frac{u_i^C}{u_i^{UC}} \right)_{i=1,\ldots,N} \tag{11}$$

$$J_2 = max. \left(\frac{v_i^C}{v_i^{UC}} \right)_{i=1,\ldots,N} \tag{12}$$

$$J_3 = max. \left(\frac{a_i^C}{a_i^{UC}} \right)_{i=1,\ldots,N} \tag{13}$$

where i is the story number and N is the number of stories in the tall building. The pseudo-code of the developed fitness function is presented in Algorithm 5.

Algorithm 5 Fitness of individuals

procedure FITNESS(benchmarkData, individualTmdAdded, excitation)
$\{u_{max}^{controlled}, v_{max}^{controlled}, a_{max}^{controlled}\}$ = MAXRESPONSE(benchmarkData, individualTmdAdded, excitation)
type $\{u_{max}^{uncontrolled}, v_{max}^{uncontrolled}, a_{max}^{uncontrolled}\}$ **as** Constant
j1 = $u_{max}^{controlled} \setminus u_{max}^{uncontrolled}$
j2 = $v_{max}^{controlled} \setminus v_{max}^{uncontrolled}$
j3 = $a_{max}^{controlled} \setminus a_{max}^{uncontrolled}$
indvFitnessAdded = [individualTmdAdded, $\{j1, j2, j3\}$]
return (indvFitnessAdded)
end procedure

5. Benchmark Building

As a case study, a 76-story, 306-meter-tall official building consisting of concrete core and concrete frames was considered. The total mass of the building was 153,000 tonnes. The initial mathematical model of the building included 76 transitional and 76 rotational degrees of freedom in which the rotational degree of freedom was then removed by the static condensation method to create a 76 degree-of-freedom model. The damping matrix of the building was calculated by considering a 1% damping ratio for the first five modes using Rayleigh's approach.

The first five natural frequencies of the building were 0.16, 0.765, 1.992, 3.79, and 6.39 Hz. The first mode shapes of the building are presented in Figure 9.

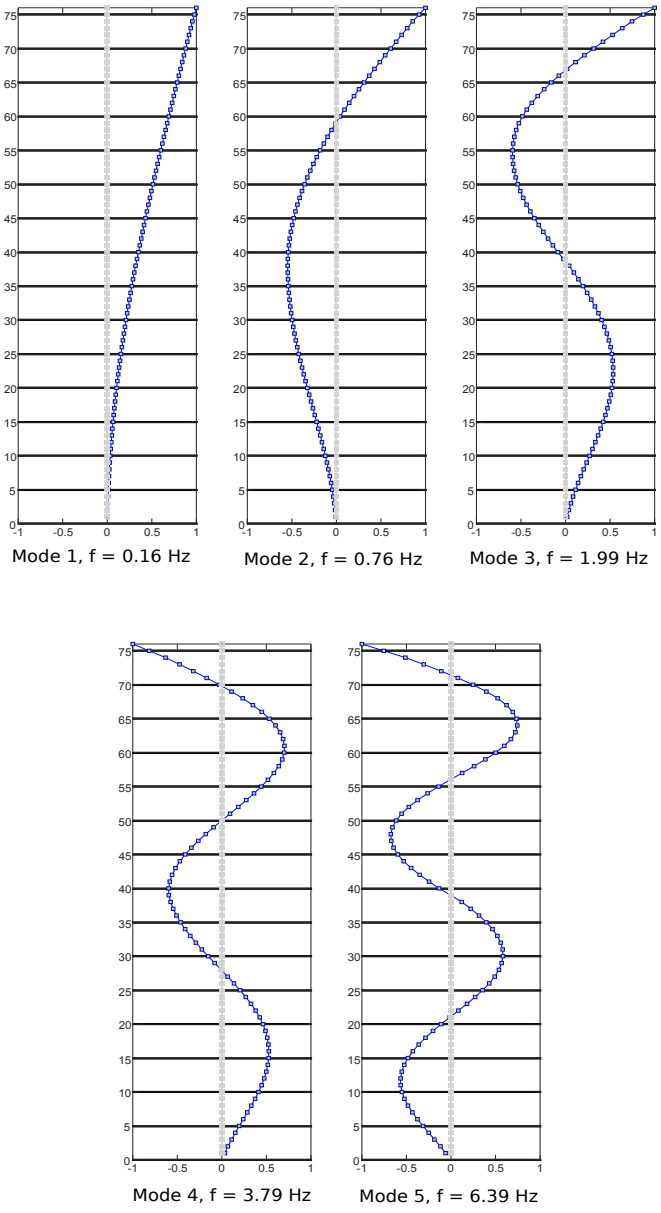

Figure 9: Five mode shapes of the 76-story building

6. Ground motion selection

In this research, the ground motions were selected and scaled using an intensity-based assessment procedure, considered according to ASCE/SEI 07-10. In this regard, seven earthquakes real acceleration records were selected from Pacific Earthquake Engineering Research (PEER) Center, NGA strong motion database [37] (see Figure 10) and then scaled using a design response spectrum. The seismic parameters and the considered design response spectrum are shown in Table 1.

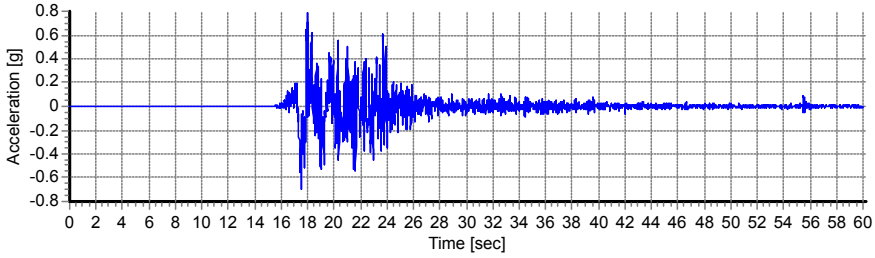

(a) Bam, 2003- Iran

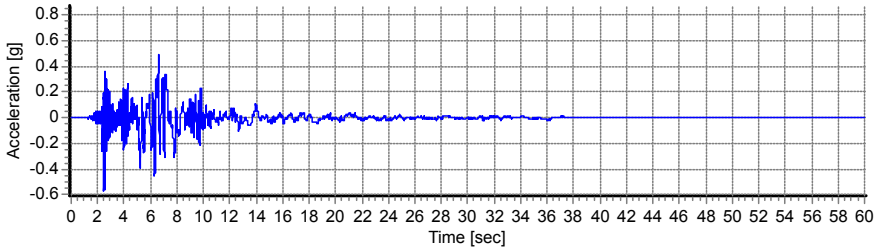

(b) Elcentro,1940- USA

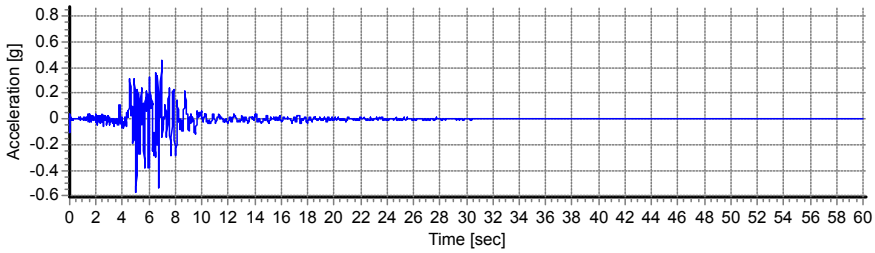

(c) Kobe, 1995- Japan

Figure 10: Earthquake acceleration records

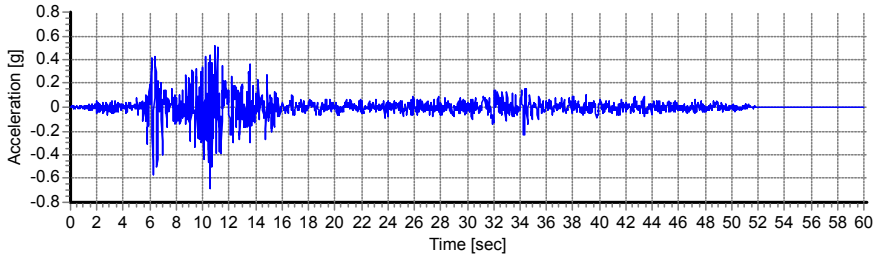

(c) Manjil, 2002, Iran

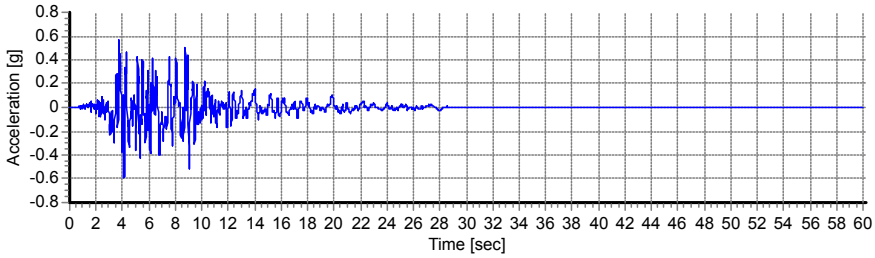

(d) Northridge, 1971- USA

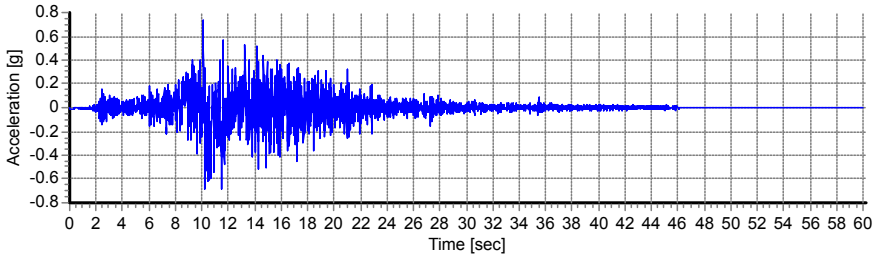

(e) Landers, 1992-USA

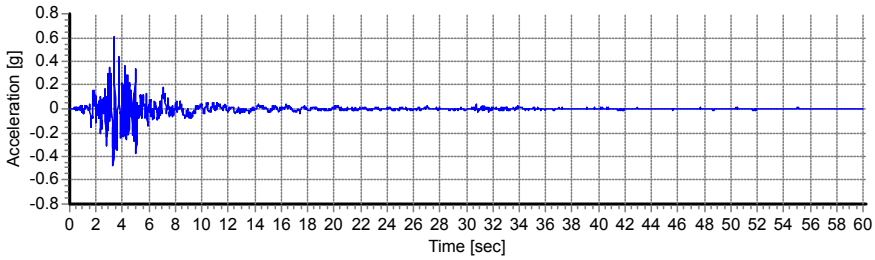

(f) SanFernando, 1994-USA

Figure 10: Earthquake acceleration records obtained from Pacific Earthquake Engineering Research (PEER) Center [37]

Accelerogram	Max. Acceleration (g)	Max. Velocity (cm/sec)	Max. Displacement (cm)	Effective Design Acceleration (g)	Predominant Period (sec)	Significant Duration (sec)
1- Bam	0.80	124.12	33.94	0.69	0.20	8.00
2- Elcentro	0.44	67.01	27.89	0.30	0.06	11.46
3- Kobe	0.31	30.80	7.47	0.28	0.42	6.20
4- Manjil	0.51	42.45	14.87	0.47	0.16	28.66
5- Northridge	0.45	60.14	21.89	0.45	0.42	10.62
6-Landers	0.72	133.40	113.92	0.52	0.08	13.15
7- SanFernando	0.22	21.71	15.91	0.20	0.00	13.15

Table 2: Original earthquakes' specifications

Accelerogram	Max. Acceleration (g)	Max. Velocity (cm/sec)	Max. Displacement (cm)	Effective Design Acceleration (g)	Predominant Period (sec)	Significant Duration (sec)
1- Bam	0.78	128.55	33.95	0.64	0.20	8.24
2- Elcentro	0.57	75.76	28.36	0.48	0.32	9.16
3- Kobe	0.56	38.83	15.68	0.56	0.36	4.16
4- Manjil	0.68	42.06	15.02	0.55	0.08	28.26
5- Northridge	0.59	64.57	22.16	0.58	0.40	10.40
6-Landers	0.73	141.02	113.78	0.56	0.08	12.92
7- SanFernando	0.60	23.71	15.88	0.61	0.10	6.03

Table 3: Scaled earthquakes' specifications

Site class	PGA	S_s	S_1	F_a	F_v	S_{MS}	S_{M1}	S_{DS}	S_{D1}
B	0.919	2.431 g	0.852 g	1	1	2.431 g	0.852 g	1.621 g	0.568 g

Table 1: Parameters of design response spectrum

The specifications of the non-scaled and scaled selected earthquakes are presented in Tables 2 and 3. The spectrum of the non-scaled and scaled excitations are shown in Figure 11.

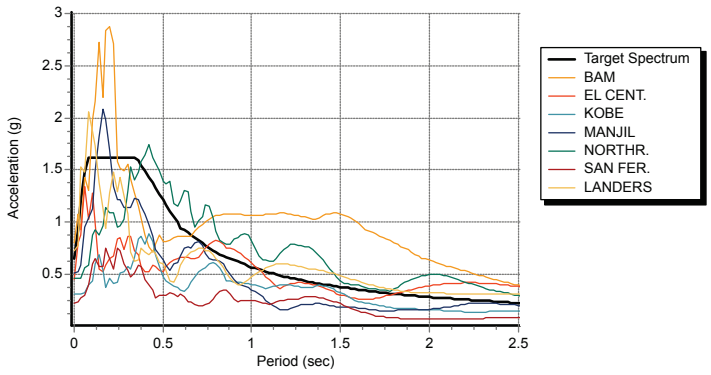

(a)

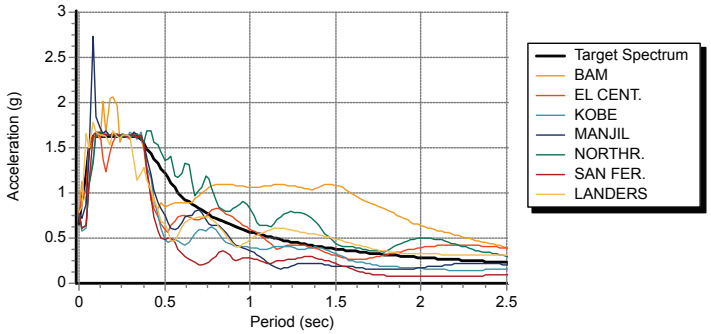

(b)

Figure 11: Respond spectrum for a. unscaled and b. scaled earthquake records

7. TMD parameters

The variation domain for m_0 , β, and ψ are considered to be in an applicable range, as shown in Table 4. The maximum value of the total mass ratio of TMDs, $m_t = \sum_{i=1}^{n} m_{0i}$, is limited to 3%, which is equal to the considered limit for each TMD. This allows the GA algorithm to either spend the allowable masses in a single TMD or divide it among multiple TMDs and distribute them over the height of the building. As is shown, the damping and the frequency ratio of the TMDs are also limited to applicable values.

Parameters	min. value	max. value
m_t	-	3%
m_0	0.2%	3%
β	0.8	1.3
ψ	5	40

Table 4: Parameters variation domain for TMDs

8. Sensitivity analysis of genetic algorithm parameters

As the parameters of GAs are highly dependent on the characteristics of each particular problem[31], the sensitivity analysis of the parameters was performed, and the optimum values were studied. Utilization of the obtained values for the GA parameters resulted in improving the quality of the solutions and the performance of the algorithm. As is shown in Table 5, during the sensitivity analysis, the crossover and mutation probabilities were iterated, and the GA results were compared for the El Centro earthquake excitation.

The results were then sorted using the NSGA sorting function and the pareto fronts were obtained as shown in Table 6. Considering the first pareto set in this table, the resultant optimum values for crossover and mutation probabilities were 0.7 and 0.2 respectively.

As a result, the parameters of the NSGA-II algorithm were considered as they are shown in Table 7. The sufficiency of 500 generations as the limit for the number of generation was then evaluated, as shown in Figure 12.

9. Optimization process

In order to study the optimum arrangement and properties of the TMD in the benchmark building, a computer code was developed based on the previously discussed theories and functions. The pseudo-code of the program is presented in Algorithm 6. In order to improve the performance of the developed code and reduce the computation time, some advanced computer programming techniques, such as parallel computing, were utilized. As a result, the code utilized multiple CPU cores to produce the multiple populations in parallel, and then all the populations were combined and sorted in each generation.

Variation No.	Crossover	Mutation	J1	J2	J3
1	0.6	0.1	0.845	0.917	0.941
2		0.2	0.860	0.926	0.950
3		0.3	0.855	0.924	0.948
4		0.4	0.839	0.915	0.942
5	**0.7**	0.1	0.862	0.925	0.946
6		**0.2**	**0.835**	**0.913**	**0.939**
7		0.3	0.861	0.925	0.947
8		0.4	0.846	0.919	0.944
9	0.8	0.1	0.869	0.929	0.950
10		0.2	0.876	0.932	0.952
11		0.3	0.842	0.915	0.941
12		0.4	0.852	0.922	0.947
13	0.9	0.1	0.871	0.930	0.951
14		0.2	0.866	0.927	0.947
15		0.3	0.874	0.932	0.953
16		0.4	0.839	0.913	0.939

Table 5: Crossover and Mutation variations

Pareto Front	Variation No.	Variation No.
1	**6**	-
2	16	-
3	4	11
4	1	-
5	8	-
6	5	12
7	3	7
8	2	14
9	9	-
10	13	-
11	10	15

Table 6: NSGA of Crossover and Mutation variations

Number of Generations	Population size	Crossover probability	Mutation probability
500	100	0.7	0.2

Table 7: NSGA II algorithm initial parameters

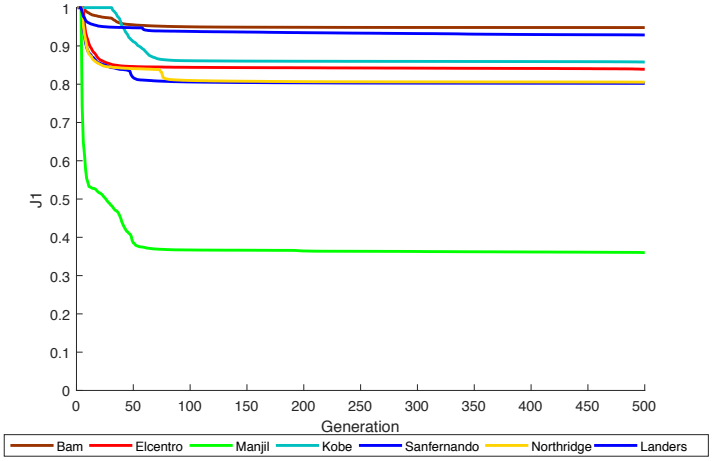

Figure 12: Trend of objectives during the generations

Algorithm 6 NSGA-II

```
population = InitializePopulation()
repeat
    repeat
        {parent1, parent2} = MakeSelection (population)
        if rnd(1) ≥ crossoverProbability
            {offspring1, offspring2} = Crossover(parent1, parent2)
            Repair(offsprint1, offspring2)
            ComputeFitness(offsprint1, offspring2)
        end if
        if rnd(1) ≥ mutationProbability
            {offspring1, offspring2} = Mutation(parent1, parent2)
            Repair(offsprint1, offspring2)
            ComputeFitness(offsprint1, offspring2)
    until size(population) ≤ M
    tempPopulation = population
    newPopulation = [ ]
    repeat
        p = ParetoFront(tempPopulation)
        ps = CrowdingDistance(p)
        newPopulation=newPopulation + ps
        tempPopulation = tempPopulation - ps
    until size(tempPopulation) > 2
    population = newPopulation
until generationNumber ≤ N
```

10. Results

The results of the optimization process, including the optimum arrangement of the TMDs and their properties, are shown in Figures 13- 19. As shown, the optimum number of TMDs is more than one for some of the excitations.

The maximum number of TMDs are three TMDs, which correspond to Bam and Manjil excitations, placed in the 76, 75, and 64 stories in both cases. Under both sets of excitations, most of the mass for the TMDs was dedicated to those on the top two stories. The tuned frequency of the TMDs was close to the fundamental frequency of the building for the top two TMDs and about 1.24 times the fundamental frequency for the TMD in the 64 story. The damping ratio of the TMDs placed on the top two stories was close to the maximum allowed value, which was 40, while it was about 14 for the TMD in the 64 story.

It was observed that the controlled displacement responses of the building improved substantially by about 65% under the Manjil earthquake excitation. On the contrary, the objective J1 for Bam earthquake had a value of about 0.95, which translated to about 5% improvement in reducing maximum displacements, compared to the uncontrolled response. This low objective value was also obtained under the Landers earthquake, with a value of about 0.93 for J1, implying 7% improvement in reducing the displacement responses. However, the displacement response shows substantial improvements in damping further oscillations compared to uncontrolled buildings.

For Landers, Northridge, and San Fernando earthquakes, the TMDs were placed on stories 76 and 74 and most of the allowed mass was dedicated to the TMD on the roof. The optimum tuning frequency of the TMDs was close to the fundamental frequency of the building. The damping values of the TMDs were between 36.39 to 39.78, which were close to the maximum considered damping ratio.

For the El Centro and Kobe earthquakes, the optimum results were obtained by placing a single TMD system on the roof. In both cases, all the allowed mass was utilized in the TMD. Under these excitations, the frequency ratios of the TMDs were registered as 1.06 and 1.05, which indicated a tuning frequency closer to the fundamental frequency of the building; the damping ratios of the TMDs were 39.53 and 39.78, which were close to the maximum allowed value.

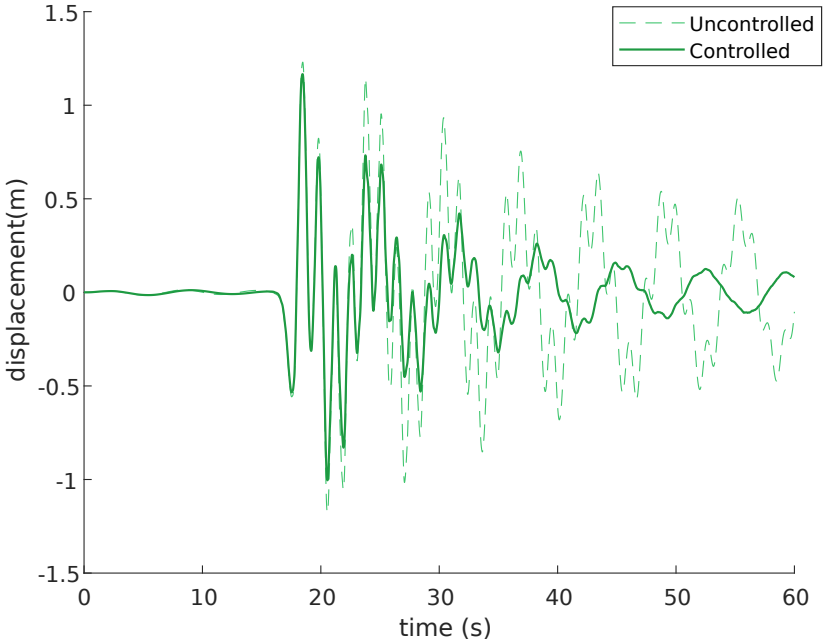

(a) Roof displacement response

Storey	m_0	β	ψ
76	1,43	0.98	39,53
75	0.93	1.01	39,46
64	0,64	1.24	18.37

(b) TMDs specifications

J1	J2	J3
0,95	0,88	0,83

(c) Objective values

Figure 13: Uncontrolled/controlled responses- Bam earthquake

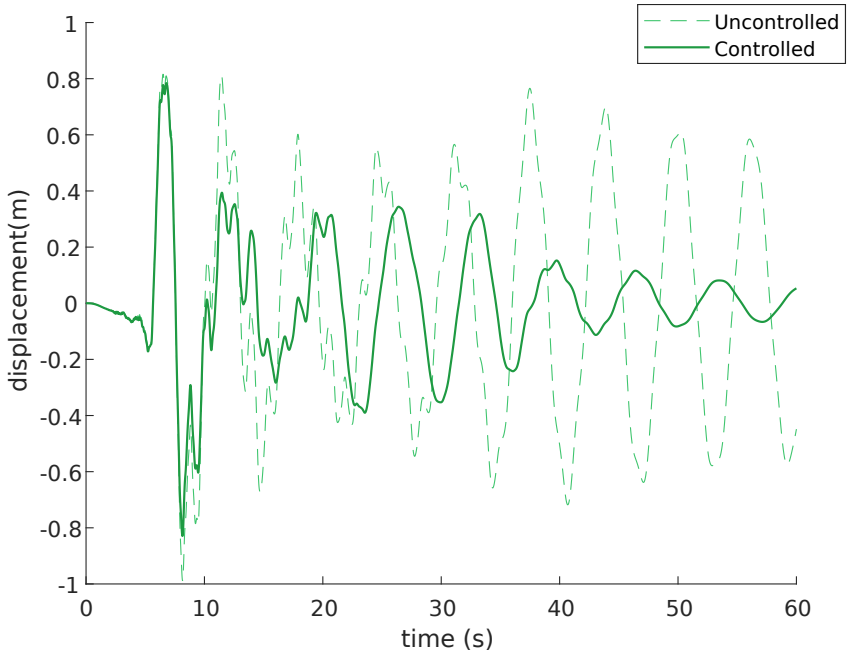

(a) Roof displacement response

Storey	m_0	β	ψ
76	2,99	1,06	39,53

(b) TMDs specifications

J1	J2	J3
0,84	0,91	0,93

(c) Objective values

Figure 14: Uncontrolled/controlled responses- Elcentro earthquake

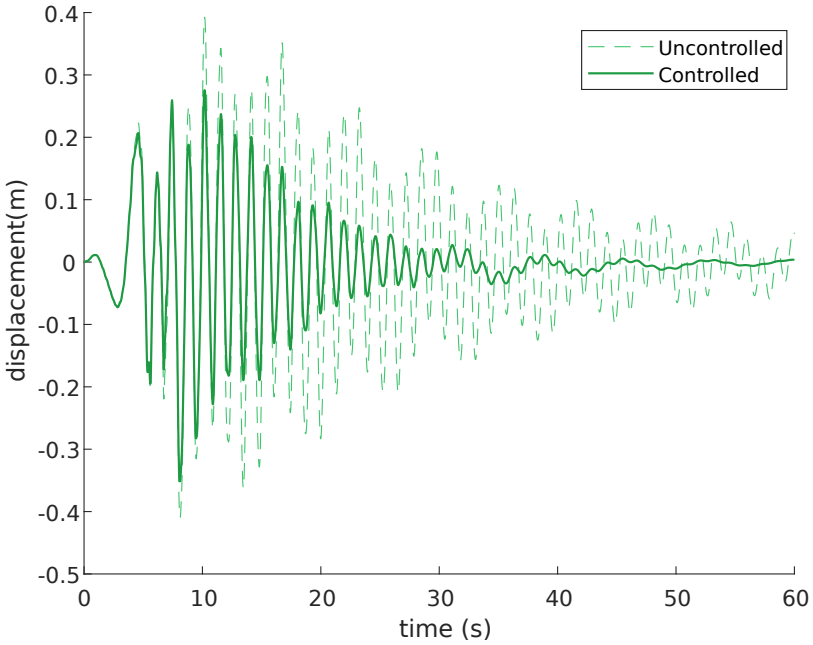

(a) Roof displacement response

Storey	m_0	β	ψ
76	3,00	1,05	39,78

(b) TMDs specifications

J1	J2	J3
0,86	0,90	0,97

(c) Objective values

Figure 15: Uncontrolled/controlled responses- Kobe earthquake

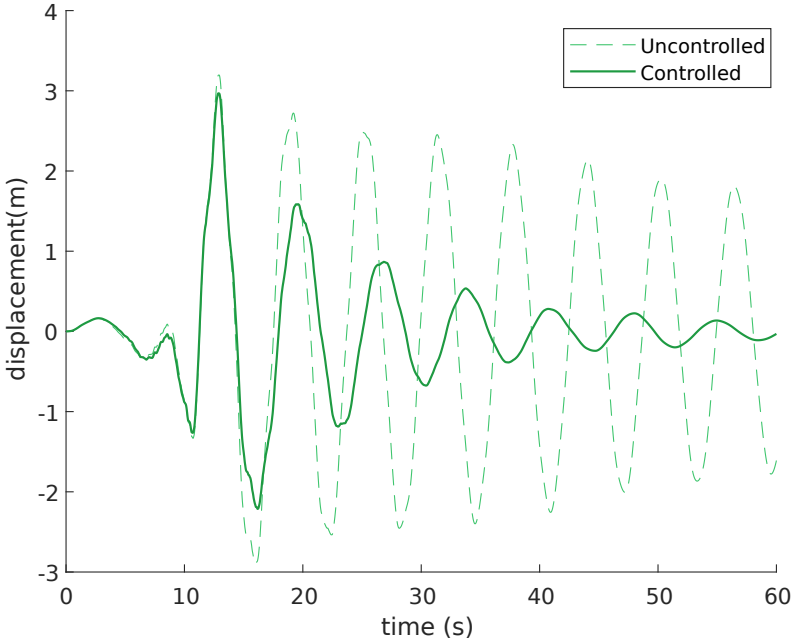

(a) Roof displacement response

Storey	m_0	β	ψ
76	2,01	1,01	37,07
74	1,00	1,01	37,13

(b) TMDs specifications

J1	J2	J3
0,93	0,89	0,98

(c) Objective values

Figure 16: Uncontrolled/controlled responses- Landers earthquake

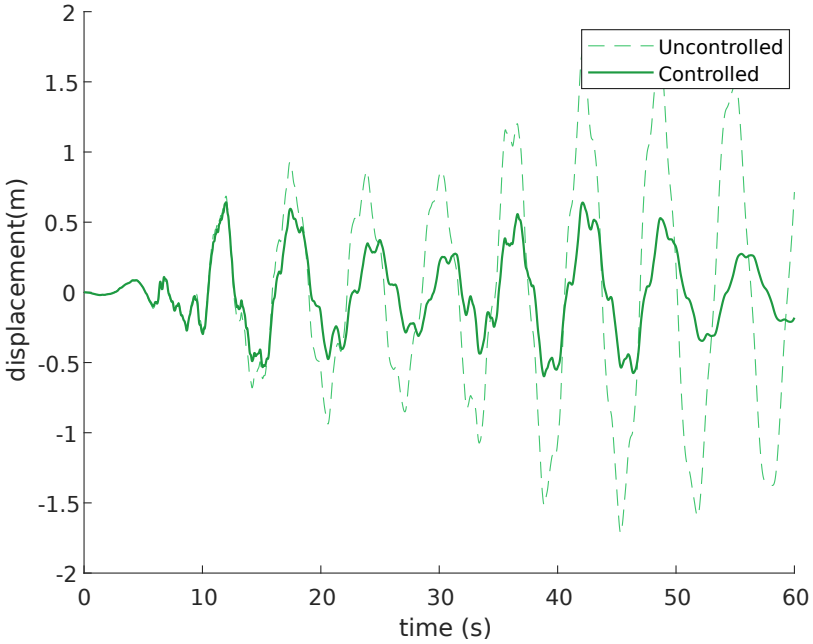

(a) Roof displacement response

Storey	m_0	β	ψ
76	1,50	1,02	35,12
75	0.95	1,01	31,34
64	0,55	1.21	14,92

(b) TMDs specifications

J1	J2	J3
0,36	0,57	0,95

(c) Objective values

Figure 17: Uncontrolled/controlled responses- Manjil earthquake

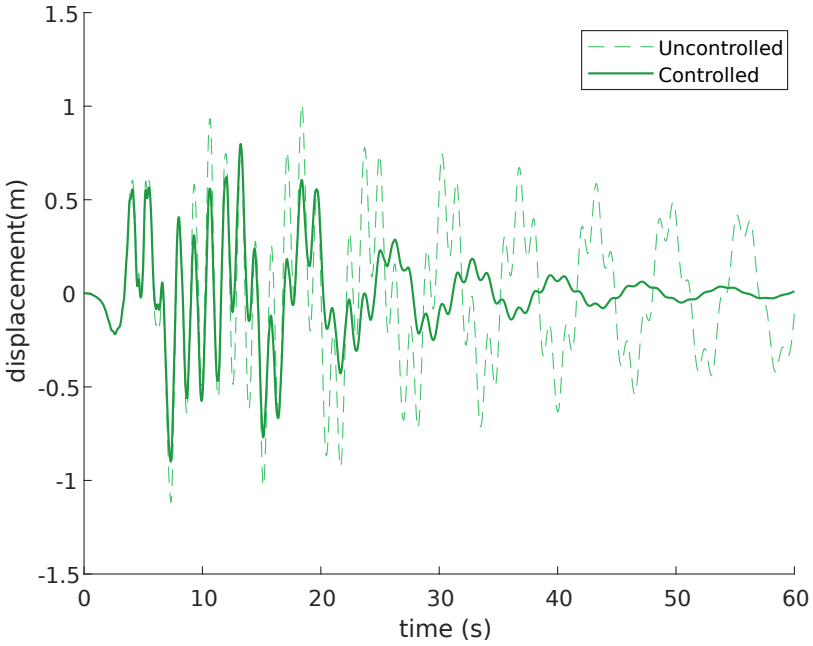

(a) Roof displacement response

Storey	m_0	β	ψ
76	2,26	1,04	37,05
74	0,75	1,04	36,98

(b) TMDs specifications

J1	J2	J3
0.81	0.84	0.95

(c) Objective values

Figure 18: Uncontrolled/controlled responses- Northridge earthquake

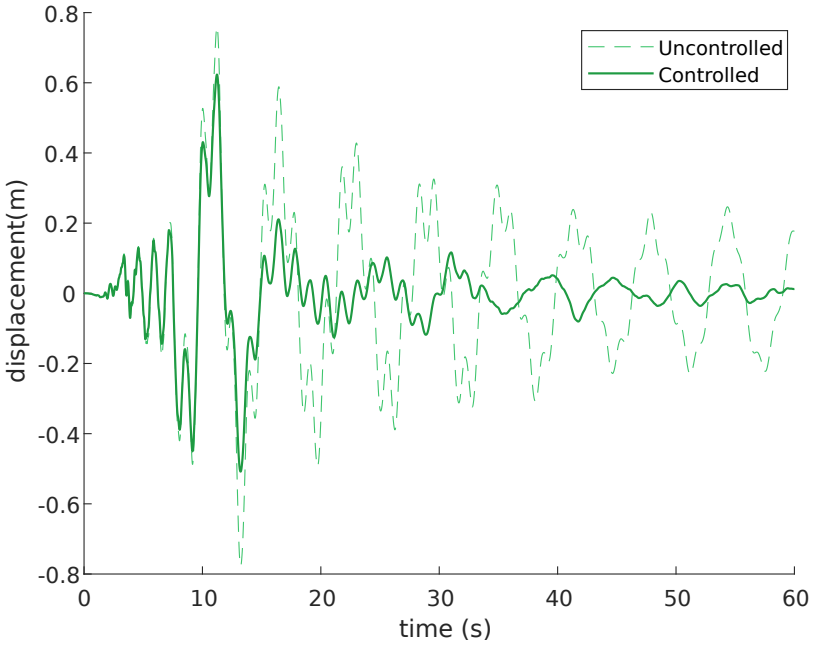

(a) Roof displacement response

Storey	m_0	β	ψ
76	2,28	1,03	36,27
74	0,72	1,03	36,39

(b) TMDs specifications

J1	J2	J3
0.80	0.84	0.97

(c) Objective values

Figure 19: Uncontrolled/controlled responses- SanFernando earthquake

11. Discussion

As mentioned in the results section, the optimum target stories for placing the TMDs included the top two stories for all of the earthquake excitations and some other stories such as 74 and 64 for some of the earthquakes. In order to understand the reasons behind this optimum arrangement, the buildings' mode shapes are again presented in Figure 20, but in each mode, the stories with maximum displacements are also marked. As shown, for the first three modes, the top three stories have the maximum displacements. For the 4th mode , the roof and the 75th and 61st stories, and for the 5th mode, the roof, and the 75th and 64th stories were the stories with maximum modal displacements.

Consequently, it can be concluded that placing a TMD on the top stories would improve the modal displacements in all five modes â an observation which agrees with the optimization results.

On the other hand, for some earthquakes, TMDs were placed in the lower stories, which implies that the optimum placement of the TMDs may also be related to some excitation properties. For this reason, Fourier transformation (FFT) was performed for each earthquake's excitation records, and the amplitudes for each building's mode frequencies were then specified to investigate the effective properties of the excitations, as shown in Figure 21. .

As shown here, unlike other earthquakes, for the Bam and Manjil earthquakes, the amplitude of the excitation in the 4th and 5th modes are more than those for the lower modes. As a result, although these higher modes have lower mass participation factors, their participation in the total response of the earthquake is increased by higher excitation amplitudes. In order to theoretically study these results, the displacement response of the building under the ground motion is presented in Equation 14 as sum of the modal nodal displacements.

$$\mathbf{u}(t) = \sum_{n=1}^{N} \mathbf{u}_n(t) \tag{14}$$

where $\mathbf{u}_n$ represents the mode nth displacements. The contribution of the nth mode to the nodal displacement $\mathbf{u}$(t) is

$$\mathbf{u_n}(t) = \phi_n q_n(t) \tag{15}$$

The q_n refers to the modal coordinate which can be calculated from following equation:

$$\ddot{q_n} + 2\zeta_n \omega_n \dot{q}_n + \omega_n^2 q_n = -\Gamma_n \ddot{u}_g(t) \tag{16}$$

In Equation 16, Γ_n is the modal participation factor of the nth mode and is the degree to which the nth mode participates in the total response. The modal participation factor can be calculated based on the modal displacements and masses as follows:

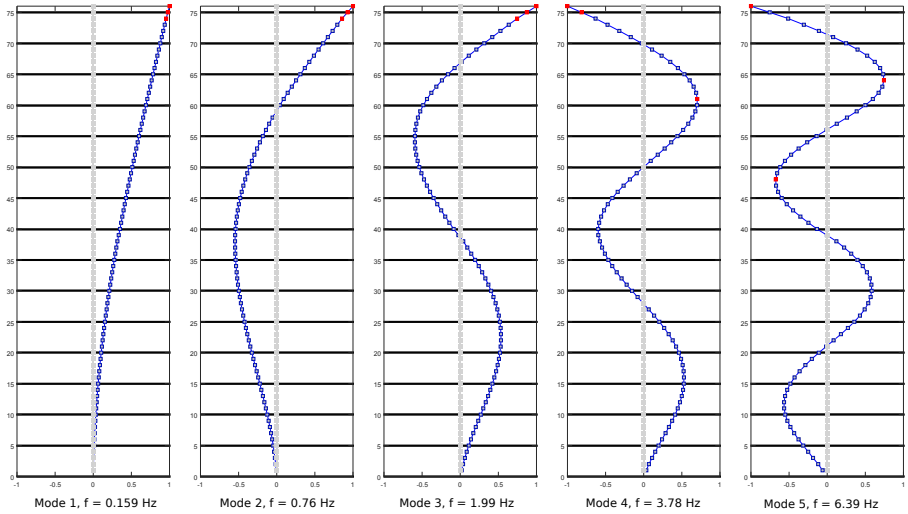

Figure 20: Three stories with maximum modal displacements in first five natural modes

$$\Gamma_n = \frac{\{\phi_n\}[M]\{1\}}{\{\phi_n\}^T[M]\{\phi_n\}} = \frac{\sum_{j=1}^{N} m_j \phi_{jn}}{\sum_{j=1}^{N} m_{jn}\phi_{jn}^2} \tag{17}$$

Equation 16 is related to a Single Degree of Freedom (SDOF) system with frequency and damping corresponding to the nth mode.

As shown here, in each mode n, the nodal displacement $\mathbf{u}_n(\mathrm{t})$ has a direct relationship with the modal displacements, ϕ_n, which means that the stories with maximum modal displacements would have greater participation in the building's modal response. In addition, it is obvious that the modal response in the nth mode is also related to the frequency content of the earthquake excitation, $\ddot{u}_g$, which means that a larger acceleration amplitude at that mode's frequency would result in lager modal responses for that mode.

Therefore, the participation of a particular story in the total response of the building would be more than the other stories if:

1. The story has maximum displacement in the modes with the larger modal participation factor.

2. The story has maximum displacement in the nth mode with the lower participation factor, but the ground motion has larger Fourier transformation amplitude in the nth mode's frequency, f_n.

These derivations validate the possibility of placing the TMDs in stories other than the top stories, a conclusion that agrees with the optimization results.

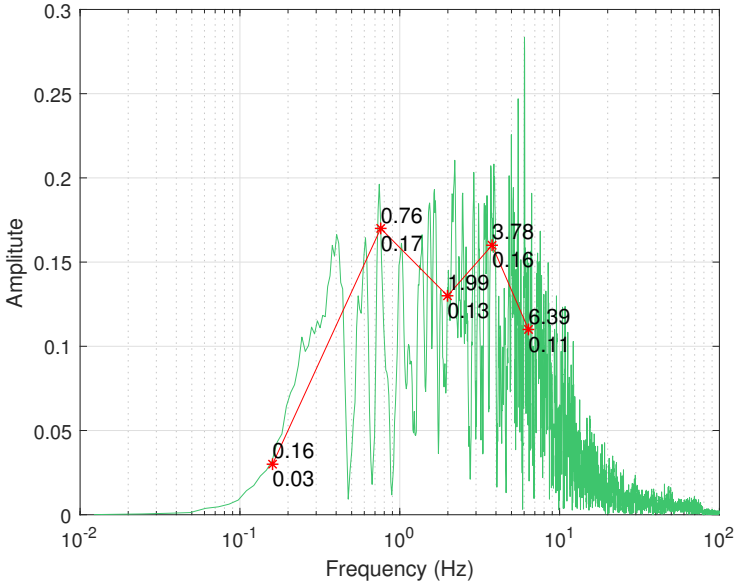

(a) Bam

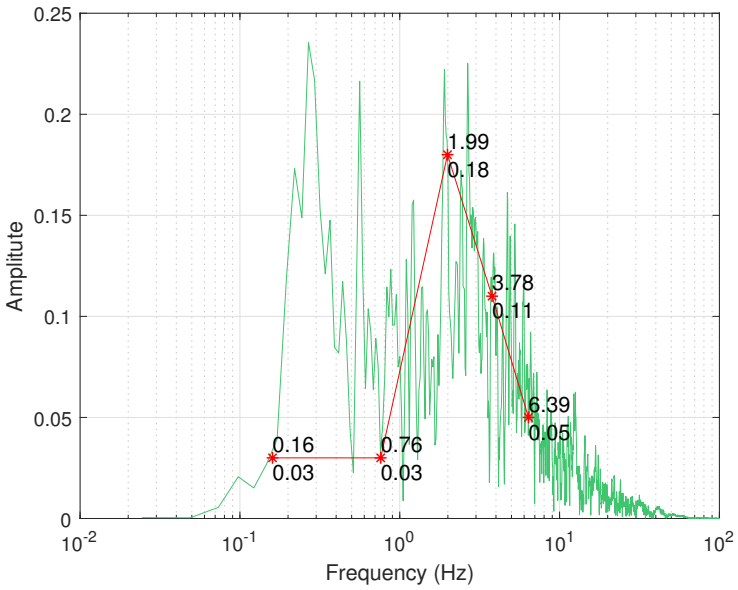

(b) Elcentro

Figure 21: Fourier transform of excitations

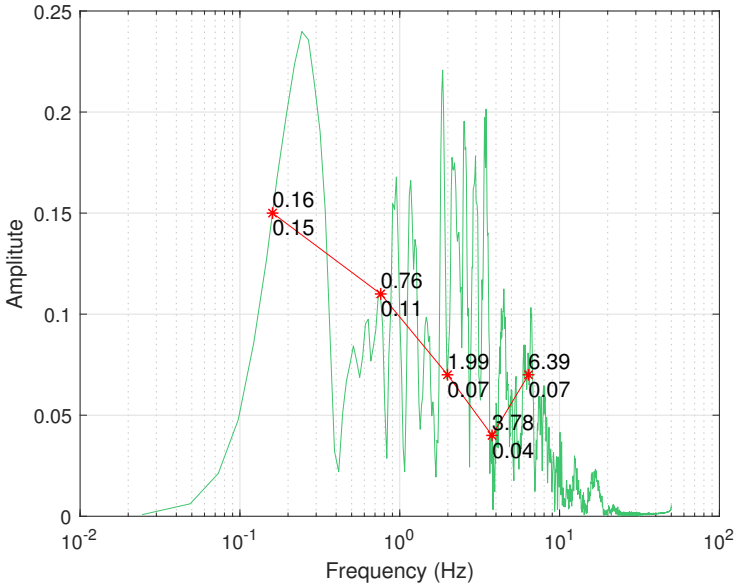

(d) Kobe

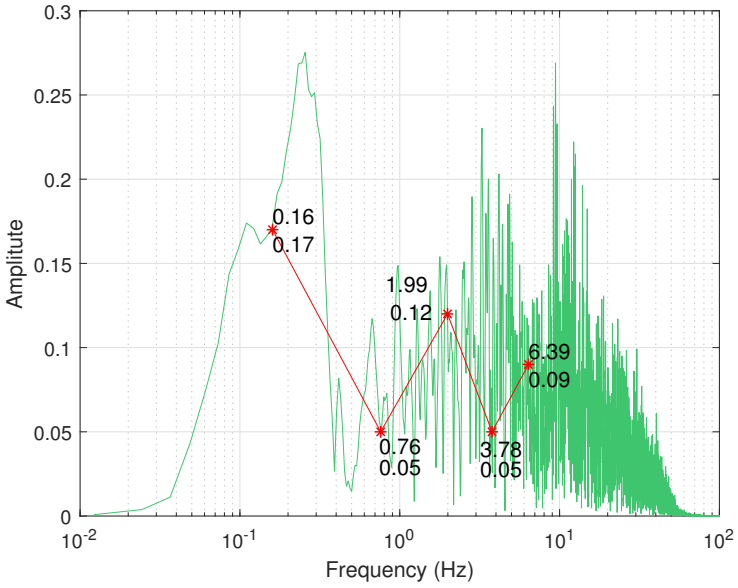

(e) Landers

Figure 21: Fourier transform of excitations

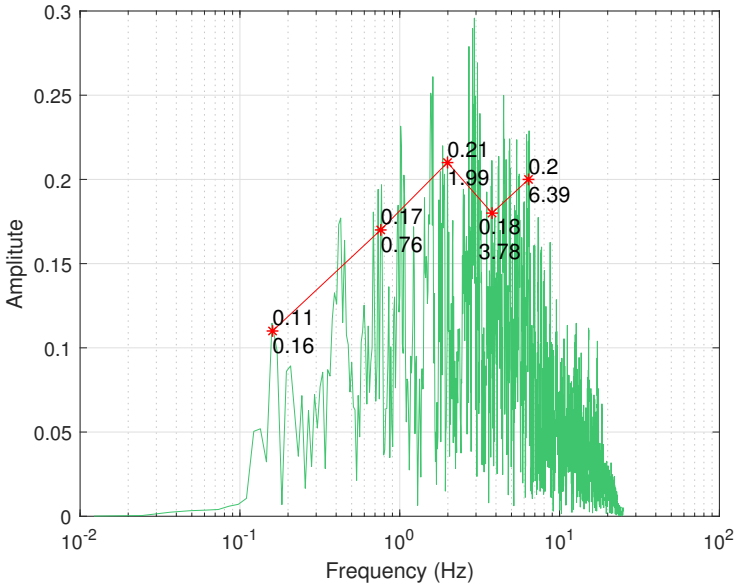

(f) Manjil

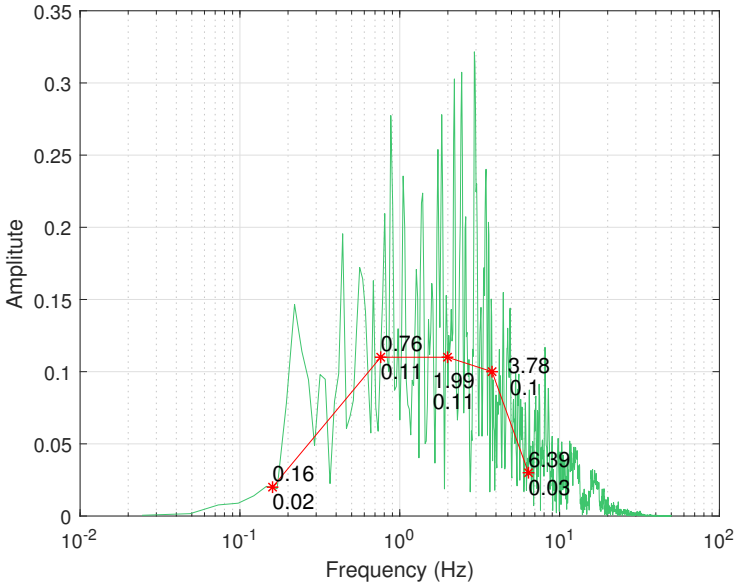

(g) Northridge

Figure 21: Fourier transform of excitations

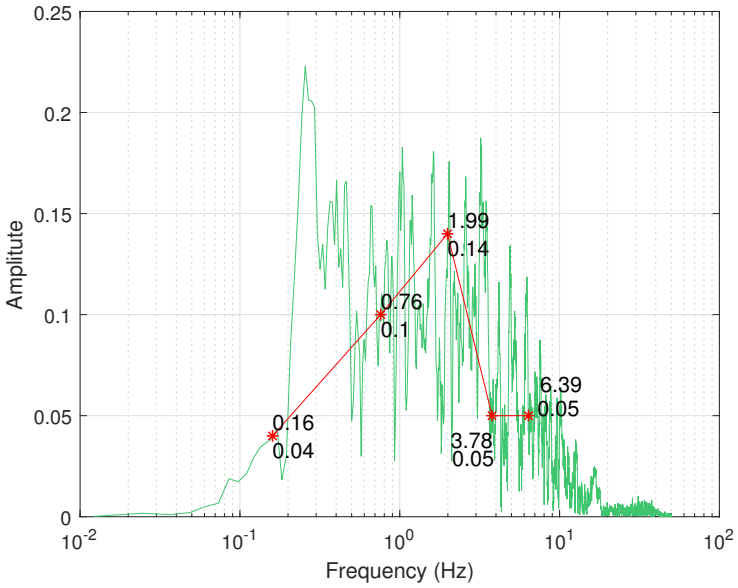

(h) San Fernando

Figure 21: Fourier transform of excitations

12. Conclusion

Considering the obtained results and related discussions in previous sections, the following conclusions can be drawn:

1. Compared to a single TMD on the roof level, a distributed multiple- TMDs system is more efficient in improving structural responses with the same amount of masses under excitation for earthquakes that have noticeable amplitude at the structure's frequencies at higher modes, a scenario likely to happen within the lifetime of a tall building.

2. The optimum placement of the TMDs include:

- The stories with maximum modal displacements in the lower structural modes.

- The stories with maximum modal displacements in modes with frequencies at which the earthquake excitation has noticeable amplitudes.

3. The optimum parameters for the TMDs that control the vibrations in the lower modes include the maximum allowed damping ratio. This indicates that increasing the damping ratio would improve the performance of such TMDs.

4. The results showed that the performance of the TMDs was not good in reducing the initial maximums in displacement responses compared to their reduction of the later maximums that occurred after some initial oscillations.

5. Even in the cases with immediate maximum displacement responses, the multiple TMDs system significantly improved the damping.

Declarations of interest

None

References

[1] Mir M. Ali and Kyoung Sun Moon. Structural Developments in Tall Buildings: Current Trends and Future Prospects. *Architectural Science Review*, 50(3):205–223, September 2007.

[2] B. F. Spencer and M. K. Sain. Controlling buildings: A new frontier in feedback. *IEEE Control Systems Magazine*, 17(6):19–35, December 1997.

[3] T. T. Soong and B. F. Spencer. Supplemental energy dissipation: State-of-the-art and state-of-the-practice. *Engineering Structures*, 24(3):243–259, March 2002.

[4] Hermann Frahm. Device for damping vibrations of bodies, April 1911.

[5] Moon Seok J., Bergman Lawrence A., and Voulgaris Petros G. Sliding Mode Control of Cable-Stayed Bridge Subjected to Seismic Excitation. *Journal of Engineering Mechanics*, 129(1):71–78, January 2003.

[6] JF Wang, CC Lin, and BL Chen. Vibration suppression for high-speed railway bridges using tuned mass dampers. *International Journal of Solids and Structures*, 40(2):465–491, 2003.

[7] Y Arfiadi and MNS Hadi. Optimum placement and properties of tuned mass dampers using hybrid genetic algorithms. *Iran University of Science & Technology*, 1(1):167–187, 2011.

[8] A. Y. T. Leung and Haijun Zhang. Particle swarm optimization of tuned mass dampers. *Engineering Structures*, 31(3):715–728, 2009.

[9] Genda Chen and Jingning Wu. Optimal Placement of Multiple Tune Mass Dampers for Seismic Structures. *Journal of Structural Engineering*, 127(9):1054–1062, 2001.

[10] Said Elias and Vasant Matsagar. Distributed Multiple Tuned Mass Dampers for Wind Vibration Response Control of High-Rise Building. *Journal of Engineering*, 2014:1–11, 2014.

[11] Chien-Liang Lee, Yung-Tsang Chen, Lap-Loi Chung, and Yen-Po Wang. Optimal design theories and applications of tuned mass dampers. *Engineering Structures*, 28(1):43–53, 2006.

[12] Chunxiang Li and Bilei Zhu. Estimating double tuned mass dampers for structures under ground acceleration using a novel optimum criterion. *Journal of Sound and Vibration*, 298(1-2):280–297, 2006.

[13] R. N. Jabary and S. P. G. Madabhushi. Tuned mass damper effects on the response of multi-storied structures observed in geotechnical centrifuge tests. *Soil Dynamics and Earthquake Engineering*, 77:373–380, 2015.

[14] Hsiang-Chuan Tsai and Guan-Cheng Lin. Optimum tuned-mass dampers for minimizing steady-state response of support-excited and damped systems. *Earthquake engineering & structural dynamics*, 22(11):957–973, 1993.

[15] Xu Y. L., Chen J., Ng C. L., and Qu W. L. Semiactive Seismic Response Control of Buildings with Podium Structure. *Journal of Structural Engineering*, 131(6):890–899, June 2005.

[16] Tharwat A. Sakr. Vibration control of buildings by using partial floor loads as multiple tuned mass dampers. *HBRC Journal*.

[17] Lei Zuo and Samir A. Nayfeh. Optimization of the Individual Stiffness and Damping Parameters in Multiple-Tuned-Mass-Damper Systems. *Journal of Vibration and Acoustics*, 127(1):77, 2005.

[18] Nam Hoang and Pennung Warnitchai. Design of multiple tuned mass dampers by using a numerical optimizer. *Earthquake Engineering & Structural Dynamics*, 34(2):125–144, 2005.

[19] M. Jokic, M. Stegic, and M. Butkovic. Reduced-order multiple tuned mass damper optimization: A bounded real lemma for descriptor systems approach. *Journal of Sound and Vibration*, 330(22):5259–5268, 2011.

[20] Alka Y. Pisal and R. S. Jangid. Seismic response of multi-story structure with multiple tuned mass friction dampers. *International Journal of Advanced Structural Engineering (IJASE)*, 6(1):1–13, 2014.

[21] Chunxiang Li and Weilian Qu. Optimum properties of multiple tuned mass dampers for reduction of translational and torsional response of structures subject to ground acceleration. *Engineering Structures*, 28(4):472–494, 2006.

[22] Tallest 10 Completed Buildings with Dampers. *CTBUH Journal*, (Issue III):48, 2018.

[23] CC Chang and WL Qu. Unified dynamic absorber design formulas for wind-induced vibration control of tall buildings. *The structural design of tall buildings*, 7(2):147–166, 1998.

[24] S. N. Deshmukh and N. K. Chandiramani. LQR Control of Wind Excited Benchmark Building Using Variable Stiffness Tuned Mass Damper. *Shock and Vibration*, 2014:1–12, 2014.

[25] S Pourzeynali, S Salimi, and H Eimani Kalesar. Robust multi-objective optimization design of TMD control device to reduce tall building responses against earthquake excitations using genetic algorithms. *Scientia Iranica*, 20(2):207–221, 2013.

[26] Nathan M. Newmark. A Method of Computation for Structural Dynamics. *Journal of the Engineering Mechanics Division*, 85(3):67–94, 1959.

[27] Melanie Mitchell. *An Introduction to Genetic Algorithms*. MIT Press, 1998.

[28] Darrell Whitley. A genetic algorithm tutorial. *Statistics and Computing*, 4(2):65–85, June 1994.

[29] Richard A. Caruana and J. David Schaffer. Representation and Hidden Bias: Gray vs. Binary Coding for Genetic Algorithms. In John Laird, editor, *Machine Learning Proceedings 1988*, pages 153–161. Morgan Kaufmann, San Francisco (CA), January 1988.

[30] N. Cohen. Fractal coding in genetic algorithm (GA) antenna optimization. In *IEEE Antennas and Propagation Society International Symposium 1997. Digest*, volume 3, pages 1692–1695 vol.3, July 1997.

[31] Mitsuo Gen and Runwei Cheng. *Genetic Algorithms and Engineering Optimization*. John Wiley & Sons, 2000.

[32] Kazi Shah Nawaz Ripon, Sam Kwong, and K. F. Man. A real-coding jumping gene genetic algorithm (RJGGA) for multiobjective optimization. *Information Sciences*, 177(2):632–654, January 2007.

[33] Günther R. Raidl and Bryant A. Julstrom. A Weighted Coding in a Genetic Algorithm for the Degree-constrained Minimum Spanning Tree Problem. In *Proceedings of the 2000 ACM Symposium on Applied Computing - Volume 1*, SAC '00, pages 440–445, New York, NY, USA, 2000. ACM.

[34] K. Deb, A. Pratap, S. Agarwal, and T. Meyarivan. A fast and elitist multiobjective genetic algorithm: NSGA-II. *IEEE Transactions on Evolutionary Computation*, 6(2):182–197, April 2002.

[35] Oliver Kramer. *Genetic Algorithm Essentials*. Springer Publishing Company, Incorporated, 1st edition, 2017.

[36] A Comparative Analysis of Selection Schemes Used in Genetic Algorithms. *Foundations of Genetic Algorithms*, 1:69–93, January 1991.

[37] PEER Ground Motion Database - PEER Center. https://ngawest2.berkeley.edu/.